Technology Enabling Circuits and Systems for the Internet-of-Things: An Overview

Johan J. Estrada-López, Amr Abuellil, Alfredo Costilla-Reyes, Edgar Sánchez-Sinencio
Electrical and Computer Engineering Department
Texas A&M University
College Station, USA
johan.estrada@tamu.edu

***Abstract* — The Internet-of-Things (IoT) network is being vigorously pushed forward from many fronts in diverse research communities. Many problems are still there to be solved, and challenges are found among its many levels of abstraction. In this paper we give an overview of recent developments in circuit design for ultra-low power transceivers and energy harvesting management units for the IoT. The study shows how this research is contributing to enable new IoT applications, by reducing active power consumption and optimizing the extraction of energy from the ambient.**

Keywords—Internet-of-Things; energy harvesting; low power

I. INTRODUCTION

The Internet-of-Things (IoT) paradigm cast a vision for the future world where everything –mobile devices, cars, electric appliances and even entire buildings– will be made "smart" and connected. With potential applications in diverse areas such as healthcare, manufacturing, agriculture, and many others [1]; it is expected that the IoT idea will affect every aspect of known human activity. However, to realize that vision many open problems have yet to be solved, creating important research challenges and opportunities across all the levels of network abstraction. One of those problems involves the dilemma of how to massively embed the desired intelligence everywhere in a practical way [2]. If indeed billions of smart "things" will eventually be deployed around the globe, what is going to be their source of energy? The many shortcomings of powering up a device only with a battery become immediately evident. To overcome those limitations, two main paths of research have been followed up from the circuits and systems perspective: the design of ultra-low power (ULP) transmitters [3], and of power management units (PMUs) for energy harvesting (EH) [4].

Fig. 1 illustrates a simple three layer model of the IoT architecture [1]. The Objects layer is mainly comprised of elements as sensors, actuators and their interfacing circuits that interact with the physical world and acquire data. The Network layer is in charge of transferring that data. Its elements include diverse technologies such as RFID, Wi-Fi and standards like Bluetooth and ZigBee. The Application layer is the one that provides diverse services to the users. The design of both ULP transmitter circuits and harvesting PMUs involve improving the performance of IoT applications across the two first layers of the architecture.

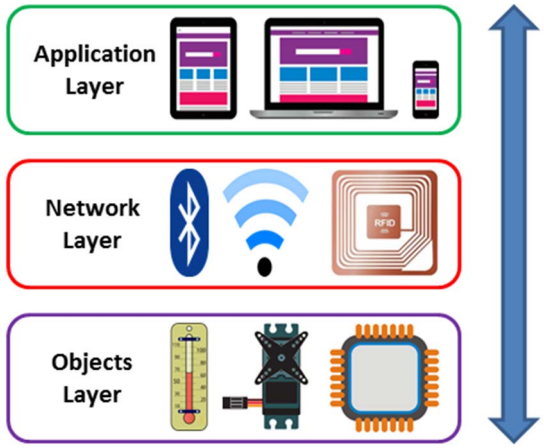

Fig. 1. An Internet-of-Things three layer architecture and their elements.

In this work, we give an overview of state-of-the-art research on both topics, and summarize the main contributions and trends. That way, a perspective can be given of the progress that has been attained and also of the areas of opportunities that still can be explored. The paper is organized as follows: Section II describes the typical architecture of an IoT sensor node and analyzes the power needs of a system created using off-the-shelf commercial components. Then, Section III will review different EH circuits and the reported power levels that can be obtained. Section IV takes a look on current work on ULP receivers and transmitters for IoT. In Section V some conclusions will be discussed.

II. TYPICAL IOT SENSOR NODE ARCHITECTURE

Fig. 2 represents the block diagram of a typical sensor node for IoT applications. As already noted, the intelligence and interaction with the physical world is provided by sensors and a microcontroller (or other type of digital processor). Data transmission is provided by a wireless unit. There is also a power management circuit that conditions the voltage coming from the battery, and delivers a regulated supply to the system. This unit also charges the battery with the energy collected by some type of transducer. For autonomous operation, the harvested energy alone should be able to provide the power consumption requirements of the complete system.

978-1-5386-4881-0/18/$31.00 ©2018 IEEE

Authorized licensed use limited to: Texas A M University. Downloaded on May 31,2020 at 00:59:15 UTC from IEEE Xplore. Restrictions apply.

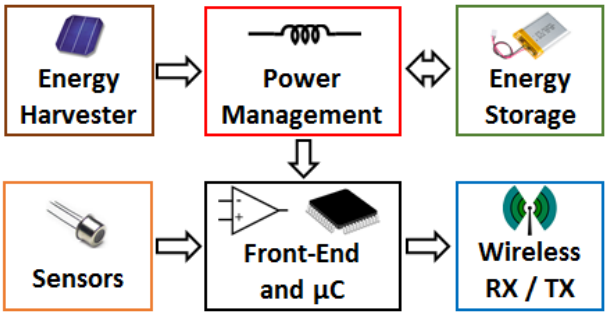

Fig. 2. Internet-of-Things sensor node diagram.

In Table I, a small sample of different commercial devices is given, covering all the main blocks of Fig. 2. The quiescent and active powers (P_Q/P_{ACT}) of these components are annotated. These values are only representative of common power needs of standard off-the-shelf components for an IoT node. From Table I, it can be observed that the minimum power consumption of a typical node with one or two sensing variables is within the range of 10's to 100's of microwatts in standby mode. For active sensing and transmission modes, the instantaneous power consumption can reach several 100's of mW. Even for a highly duty-cycled operation of the node, this amount of instantaneous power must still be available from the energy storage element (battery or supercapacitor) to meet the demands of the system.

TABLE I. POWER CONSUMPTION OF SAMPLE COMMERCIAL DEVICES FOR IOT

Device	*Type*	P_Q / P_{ACTV}
SHTW2 [5]	RH sensor	1.26µW / 8.6µW
CC3200 [6]	µC with Wi-Fi	13.2µW / 756µW
XB24-AWI-001 [7]	Zigbee RX/TX	10µW / 148mW
BQ25570 [8]	PMIC with EH	2.1nW / 1mW
TLVx333 [9]	CMOS Op Amp	30µW / N.A.

In the sensor node system of Fig. 2, there are many critical points where optimization can be performed to increase its lifetime [10]. Improvements in the PMU involves an increased harvested energy and better power conversion efficiency. In the case of the wireless unit, low-voltage operation and decreased power consumption are commonly the targeted goals. In the two following sections we explore how these improvements are being achieved in state-of-the-art research.

III. ENERGY HARVESTING FOR IOT

Fig. 3 shows the general architecture of an autonomous power management unit for energy harvesting. The purpose of the cold start-up circuit is enabling the whole system to start operating, even when zero energy is initially available at the storage element. Many times this block is implemented using a very inefficient secondary converter, able to operate at extremely low values of input voltage. Once the undervoltage-lockout (UVLO) detects that the output voltage exhibits the minimum operating value for the system, it sends the control signals to the main DC-DC converter to start its operation.

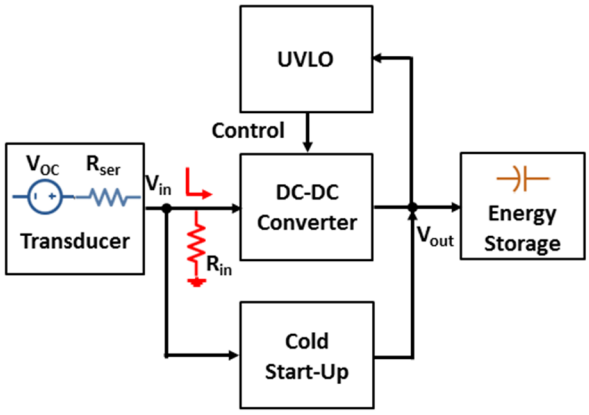

Fig. 3. General architcture of an autonomous energy harvesting PMU.

The main switching DC-DC converter can be a capacitive-based [11]-[15], [17], [21] or inductive-based [16], [18]-[20] topology. Generally, inductive switching converters have been designed to be able to start harvesting power from voltages as low as 50mV [19]. Also, circuit design techniques for nanoampere current consumption in these type of converters allows them to harvest power from inputs as low as 300nW or 1µW [11], [16]. On the other side, charge pump designs require minimum input voltages from 200 to 400mV [15], [20]. However, switched-inductor converters require an off-chip component in order to show acceptable efficiency levels, while switched-capacitor topologies can be fully integrated with similar performance in terms of efficiency.

In order to ensure the maximum transfer of energy from the transducer to the storage element, the DC-DC converter does not only need to be highly efficient, but also be able to ensure maximum power point tracking (MPPT). That means that the input impedance seen at the switched converter (R_{in}) matches the equivalent output series resistance (R_{ser}) of the harvester, and also tracks its changes over time for different ambient conditions. In this type of applications, inductive converters typically operate in Discontinuous Conduction Mode (DCM), due to the low current levels that are handled. In that case, R_{in} control can be made by varying the switching frequency of the converter, through Pulse Frequency Modulation (PFM) [16], [20]. Switched-capacitor converters can have two-dimensional control over their equivalent input resistance by tuning the switching frequency and also reconfiguring their conversion ratio [15].

As shown in Fig. 4, several techniques to perform MPPT have been proposed. One of them (Fig. 4(a)) is the fractional open circuit voltage (FOCV) method, which requires a sampling of the open circuit voltage (V_{OC}) from the transducer and then tuning the DC-DC converter until its input voltage is a fraction of that sample, i.e. $V_{in} = K_{MPPT} \cdot V_{OC}$ [17]. The value of K_{MPPT} depends on the type of transducer and has been empirically found to be ≈ 0.8 and 0.5 for photovoltaic and thermal harvesters, respectively. Fig. 4(b) depicts another MPPT method that applies a hill-climbing algorithm, where the output voltage V_{sto} is continuously monitored while tuning the switching converter. In this case the algorithm searches for a global maximum in the output power for specific operating conditions of the transducer [15]. Finally, as shown in Fig. 4(c)

978-1-5386-4881-0/18/$31.00 ©2018 IEEE

Authorized licensed use limited to: Texas A M University. Downloaded on May 31,2020 at 00:59:15 UTC from IEEE Xplore. Restrictions apply.

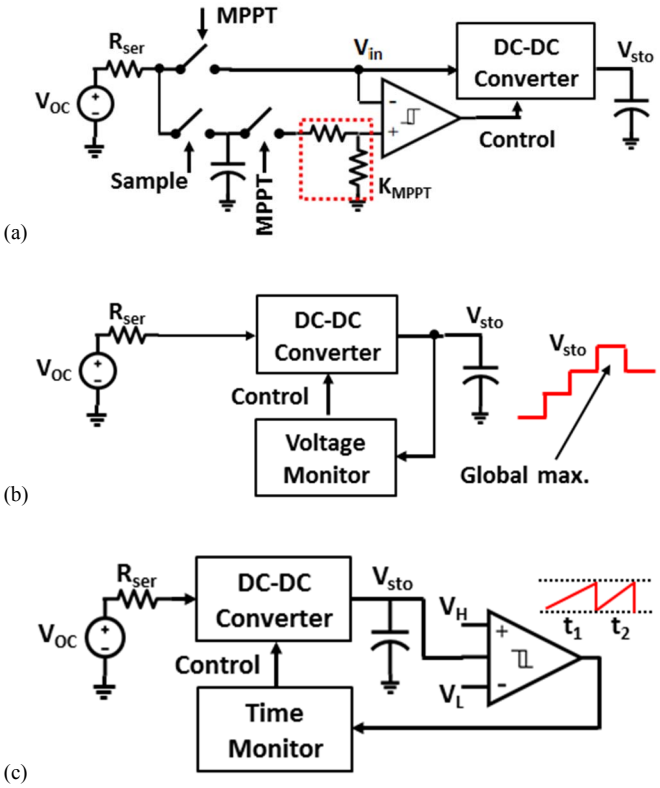

Fig. 4. Maximum power point tracking techniques: (a) Fractional open circuit voltage, (b) Hill-climbing algorithm and (c) time-based method.

other works have proposed indirect time-based methods to perform MPPT [14]; like measuring the time it takes for the output voltage to charge the storage capacitor between to predefined levels. Table II summarize all the mentioned MPPT techniques, contrasting their main advantages and disadvantages.

TABLE II. MPPT METHODS COMPARISON

Method	*Advantages*	*Disadvantages*
Fractional open circuit voltage	Good trade-off between converted and consumed power.	Limited tracking accuracy.
Hill-climbing algorithim	Good tracking accuracy.	Continuous monitoring can increases power consumption overhead
Indirec time based	Good tracking accuracy and output voltage regulation.	Increased design complexity.

Fig. 5 illustrates the progress over the last seven years in terms of available output power for several energy harvesting PMUs. Often is hard to compare these results in a meaningful way due to the fact that most of the works don't follow a standard methodology in the characterization of their designs: transducers vary from one work to another, different test conditions (i.e. illumination, temperature gradient, mechanical acceleration) are used in the measurements, among other factors. However, a relatively fair comparison can be done by stablishing a unifying criterion. For example, mostly a common architecture is selected for each type of transducer: capacitive and inductive based converters for solar and thermal

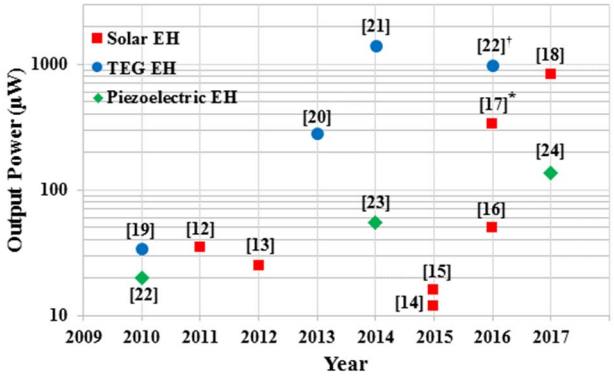

Fig. 5. Output power trends in energy harvesting power management units.

harvesters, respectively; and the synchronized-switch harvesting on inductor (SSHI) technique for piezoelectric transducer. Also, the output power is always taken with reference to the maximum efficiency that is reported for each design. With these basic criteria, it is possible to trace the evolution of a particular technique or topology and observe how the particular contributions of each work advances circuit performance over time. From Fig. 5 it can be seen that in general, there is a trend of increased available output power, and that state-of-the-art designs can already deliver from 100's of µW to a couple of mW of instantaneous power, satisfying the minimum requirements of consumed energy in standby mode of a typical sensor node.

IV. ULP RX/TX CIRCUITS AND SYSTEMS

Achieving efficient wireless communication between nodes is not a unique function of reducing the power consumption of all the circuits that are involved. Network synchronization and node start-up time have proven to be as equally important [25]. Network synchronization leads to extra power consumption, especially in the cases of small payloads and heavily duty-cycled systems. However, some sort of synchronization is required as there is no guarantee that the receiver (*RX*) is listening at the same time the transmitter (*TX*) is sending data. The simplest method would be "preamble synchronization," which requires the transmitter to send a certain repetitive pattern; to queue the receiver to start receiving data. A major drawback clearly shows up for duty-cycled systems, as sending a single data package of a few bytes (i.e. < 1ms at moderate data rates) with a receiver that wakes up once every minute to sense the channel, requires a transmitter to send a preamble longer than a minute to insure synchronization. It can be noted that saving power at the receiver side by further duty-cycling impacts the transmitter consumption, creating an unequal link-budget and increasing the synchronization power overhead.

To solve the problems created by preamble synchronization, wake-up radio functionality has been proposed for modern wireless networks. The implementation can be as simple as a wake-on RF power topology as shown in [26]. Though very efficient at the circuit level, in most practical cases (congested networks or co-existence of multiple standards) it still cannot achieve high network efficiency, due to the occurrence of false wake-ups. To avoid this behavior, [27] designed a circuit allowing a single receiver to wake-up when a unique on-off (OOK) keying pattern is recognized.

978-1-5386-4881-0/18/$31.00 ©2018 IEEE

Authorized licensed use limited to: Texas A M University. Downloaded on May 31,2020 at 00:59:15 UTC from IEEE Xplore. Restrictions apply.

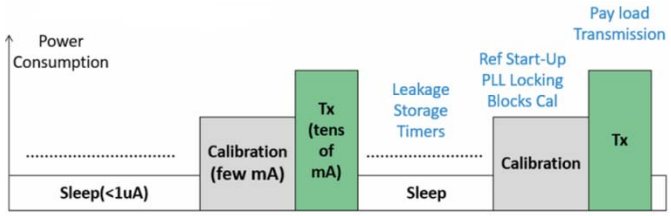

Fig. 6. Typical node current consumtpion in IoT applications.

A more extensive survey of wake-up circuits and their various categories is presented in [28]. It is important to observe that the majority of these wake-up techniques cannot be integrated as part of conventional wireless standards (Bluetooth LE, Wi-Fi). However, recent work shows that enhancing these standards is a possibility through a custom media access control (MAC) layer [29].

As already mentioned, node start-up time is another factor degrading the communication efficiency, this time at the chip level. Fig. 6 shows a typical node power consumption pattern. After waking up from a sleep state just before enabling transmission, the circuit goes through start-up and calibration phases. The spectral efficiency and channel accuracy requirements dictate a highly precise frequency reference in the circuit, within a few ppm. A phase locked loop (PLL) with a crystal oscillator (XO) is commonly used to provide such accuracy. However, the high quality factor Q (~10,000) of the crystal and the low bandwidth (BW) of the PLL (for noise rejection and stability) drastically increase the start-up and locking times respectively. The *TX*/*RX* cycle efficiency must take into consideration the energy that is lost in states prior transmission. Equation (1) justifies the need for minimizing the energy consumed in sleep state (E_{Sleep}) and calibration/start-up time (E_{Cal}), as in most practical cases the integration of their power exceeds the energy spent during transmission ($E_{TX/RX}$).

$$\text{Energy per bit} = \frac{E_{Sleep}+E_{Cal}+E_{Tx/Rx}}{No.\ of\ bits\ transmitted}\ \frac{J}{Bit} \qquad (1)$$

The calibration phase is dominated by the XO start-up time (≈ 1ms for MHz crystals). This period is a function of the initial noise seed in the crystal and the amount of negative impedance that is applied from the oscillator core to grow this noise seed into a sustained oscillation. In [30] a form of noise injection is proposed using a high resolution pre-calibrated ring oscillator (RO) exactly at the crystal frequency, which in practice is hard to do considering temperature variations: with a high Q for the crystal, any frequency shifted from its resonance will not enhance the noise seed. To reduce such complexity, [31] proposes a chirp method to scan all the frequencies around the crystal frequency, guaranteeing that the chirp frequency will cross the crystal frequency through the control ramp time, in addition to negative resistance boosting during start-up. Finally, [32] characterized the effect of noise injection time (via a RO) vs the achieved start-up time reducing it by a further 15x from the previous techniques, but still the complexity of temperature compensation for the RO is needed for precise frequency.

PLL locking time reduction is usually done by manipulating the PLL loop BW as in [33], or using a dynamic phase detector with auxiliary charge pump as in [34]. Another approach for faster start-up is through architecture make-over: removing the PLL and replacing it with a direct injection locking from the XO [35], or using digital calibration for the RO prior transmission as in [36].

Finally, at the circuit level block stacking has been a trend for more than 10 years, reusing the current in a branch by making it pass through other blocks stacked below on the same supply. In [37] a stacked voltage-controlled oscillator (VCO) was implemented over multiple RF blocks, reusing the current needed for the VCO by making it pass through the low noise amplifier (LNA), intermediate frequency (IF) amplifier and power amplifier (PA). This distributed stacking maximizes the use of the 3V supply to provide headroom for these blocks, eliminating the need for a high efficiency buck converter to supply multiple low voltages. Instead, the main battery was used directly achieving a power consumption of 1.3mW for a -6dBm output power and -94dBm *RX* sensitivity. The same technique was used recently in [38], but also incorporated a mitigation of the "VCO Pulling" effect. This effect usually happens by load pulling, coupling through substrate/supply or by magnetic coupling, since the VCO and PA are on the same frequency with no proper isolation in between. In [38] isolation is implemented by separating current mirrors for each block and other techniques, as very strong AC grounding for the common point and most importantly; adding a resistive buffer on the same stack to avoid the PA internal matching network from affecting the VCO tank. In [27] stacking was used inside the PLL for VCO and quadrature divider with the VCO running on double frequency to avoid pulling effects.

V. Conclusions

The recent developments in circuit and system design for energy harvesting and ultra-low power wireless transmitters play a key role in enabling many IoT applications that in the past couldn't be made possible. However, there is still a long way to go in terms of maximum extracted energy, power efficiency and low-voltage operation. In the case of energy harvesting, improvements are needed not only at the circuit level but also in terms of transducer technology, to be able to comply with the power requirements of sensor nodes in the active modes of sensing and data transmission, without the need of recurring to heavy duty-cycling; which also creates problems at the Network level. In the case of ULP transmitters for wireless sensor networks applications, the reduction of power consumption requirements is a problem that must be addressed on many levels, in order to finally reach the reality of completely autonomous network operation with energy harvesting as the only source of power.

Acknowledgment

This work was supported in part by Intel, Qualcomm, Texas Instruments, CONACYT and UADY.

References

[1] A. Al-Fuqaha, M. Guizani, M. Mohammadi, M. Aledhari and M. Ayyash, "Internet of Things: A Survey on Enabling Technologies, Protocols, and Applications," in *IEEE Communications Surveys & Tutorials*, vol. 17, no. 4, pp. 2347-2376, Fourthquarter 2015.

978-1-5386-4881-0/18/$31.00 ©2018 IEEE

Authorized licensed use limited to: Texas A M University. Downloaded on May 31,2020 at 00:59:15 UTC from IEEE Xplore. Restrictions apply.

[2] J. A. Stankovic, "Research Directions for the Internet of Things," in *IEEE Internet of Things Journal*, vol. 1, no. 1, pp. 3-9, Feb. 2014.

[3] A. Burdett, "Ultra-Low-Power Wireless Systems: Energy-Efficient Radios for the Internet of Things," in *IEEE Solid-State Circuits Magazine*, vol. 7, no. 2, pp. 18-28, Spring 2015.

[4] R. J. M. Vullers, et.al., "Energy Harvesting for Autonomous Wireless Sensor Networks," in *IEEE Solid-State Circuits Magazine*, vol. 2, no. 2, pp. 29-38, Spring 2010.

[5] Sensirion, "WLCSP Humidity and Temperature Sensor IC," SHTW2 datasheet, Jul. 2017.

[6] Texas Instruments, "CC3200 SimpleLink™ Wi-Fi® and Internet-of-Things Solution, a Single-Chip Wireless MCU," CC3200 datasheet, Jul. 2013 [Revised Feb. 2015].

[7] Digi International, "Digi Xbee® S1 802.15.4 RF modules," XB24-AWI-001 datasheet.

[8] Texas Instruments, "Nano Power Boost Charger and Buck Converter for Energy Harvester Powered Applications," BQ25570 datasheet, Mar. 2015.

[9] Texas Instruments, "TLVx333 2-μV V_{OS}, 0.02-μV/°C, 17-μA, CMOS Operational Amplifiers Zero-Drift Series," TLVx333 datahseet, Dec. 2015.

[10] N. Shafiee, S. Tewari, B. Calhoun and A. Shrivastava, "Infrastructure Circuits for Lifetime Improvement of Ultra-Low Power IoT Devices," in *IEEE Transactions on Circuits and Systems I: Regular Papers*, vol. 64, no. 9, pp. 2598-2610, Sept. 2017.

[11] G. Chowdary and S. Chatterjee, "A 300-nW Sensitive, 50-nA DC-DC Converter for Energy Harvesting Applications," in *IEEE Transactions on Circuits and Systems I: Regular Papers*, vol. 62, no. 11, pp. 2674-2684, Nov. 2015.

[12] J. Kim, J. Kim and C. Kim, "A Regulated Charge Pump With a Low-Power Integrated Optimum Power Point Tracking Algorithm for Indoor Solar Energy Harvesting," in *IEEE Transactions on Circuits and Systems II: Express Briefs*, vol. 58, no. 12, pp. 802-806, Dec. 2011.

[13] P. H. Chen *et al*., "An 80 mV Startup Dual-Mode Boost Converter by Charge-Pumped Pulse Generator and Threshold Voltage Tuned Oscillator With Hot Carrier Injection," in *IEEE Journal of Solid-State Circuits*, vol. 47, no. 11, pp. 2554-2562, Nov. 2012.

[14] X. Liu and E. Sánchez-Sinencio, "An 86% Efficiency 12 μW Self-Sustaining PV Energy Harvesting System With Hysteresis Regulation and Time-Domain MPPT for IOT Smart Nodes," in *IEEE Journal of Solid-State Circuits*, vol. 50, no. 6, pp. 1424-1437, June 2015.

[15] X. Liu and E. Sánchez-Sinencio, "A Highly Efficient Ultralow Photovoltaic Power Harvesting System With MPPT for Internet of Things Smart Nodes," in *IEEE Transactions on Very Large Scale Integration (VLSI) Systems*, vol. 23, no. 12, pp. 3065-3075, Dec. 2015.

[16] X. Liu, L. Huang, K. Ravichandran and E. Sánchez-Sinencio, "A Highly Efficient Reconfigurable Charge Pump Energy Harvester With Wide Harvesting Range and Two-Dimensional MPPT for Internet of Things," in *IEEE Journal of Solid-State Circuits*, vol. 51, no. 5, pp. 1302-1312, May 2016.

[17] M. Dini, A. Romani, M. Filippi and M. Tartagni, "A Nanocurrent Power Management IC for Low-Voltage Energy Harvesting Sources," in *IEEE Transactions on Power Electronics*, vol. 31, no. 6, pp. 4292-4304, June 2016.

[18] S. Mondal and R. Paily, "On-Chip Photovoltaic Power Harvesting System With Low-Overhead Adaptive MPPT for IoT Nodes," in *IEEE Internet of Things Journal*, vol. 4, no. 5, pp. 1624-1633, Oct. 2017.

[19] E. J. Carlson, K. Strunz and B. P. Otis, "A 20 mV Input Boost Converter With Efficient Digital Control for Thermoelectric Energy Harvesting," in *IEEE Journal of Solid-State Circuits*, vol. 45, no. 4, pp. 741-750, April 2010.

[20] P. S. Weng, et.al., "50 mV-Input Batteryless Boost Converter for Thermal Energy Harvesting," in *IEEE Journal of Solid-State Circuits*, vol. 48, no. 4, pp. 1031-1041, April 2013.

[21] S. Carreon-Bautista, A. Eladawy, A. Nader Mohieldin and E. Sánchez-Sinencio, "Boost Converter With Dynamic Input Impedance Matching for Energy Harvesting With Multi-Array Thermoelectric Generators," in *IEEE Transactions on Industrial Electronics*, vol. 61, no. 10, pp. 5345-5353, Oct. 2014

[22] Y. K. Ramadass and A. P. Chandrakasan, "An Efficient Piezoelectric Energy Harvesting Interface Circuit Using a Bias-Flip Rectifier and Shared Inductor," *IEEE J. Solid-State Circuits*, vol. 45, no. 1, pp. 189–204, Jan. 2010.

[23] E. E. Aktakka and K. Najafi, "A Micro Inertial Energy Harvesting Platform with Self-supplied Power Management Circuit for Autonomous Wireless Sensor Nodes," *IEEE J. Solid-State Circuits*, vol. 49, no. 9, pp. 2017–2029, Sep. 2014.

[24] L. Wu, X. D. Do, S. G. Lee and D. S. Ha, "A Self-Powered and Optimal SSHI Circuit Integrated With an Active Rectifier for Piezoelectric Energy Harvesting," in *IEEE Transactions on Circuits and Systems I: Regular Papers*, vol. 64, no. 3, pp. 537-549, March 2017.

[25] Texas Instruments, "Low Power RF Designer's Guide to LPRF," SLYA020a Application Note, 2010.

[26] N. E. Roberts and D. D. Wentzloff, "A 98nW wake-up radio for wireless body area networks," *2012 IEEE Radio Frequency Integrated Circuits Symposium*, Montreal, QC, 2012, pp. 373-376.

[27] Y. I. Kwon, S. G. Park, T. J. Park, K. S. Cho and H. Y. Lee, "An Ultra Low-Power CMOS Transceiver Using Various Low-Power Techniques for LR-WPAN Applications," in *IEEE Transactions on Circuits and Systems I: Regular Papers*, vol. 59, no. 2, pp. 324-336, Feb. 2012.

[28] R. Piyare, A. L. Murphy, C. Kiraly, P. Tosato and D. Brunelli, "Ultra Low Power Wake-Up Radios: A Hardware and Networking Survey," in *IEEE Communications Surveys & Tutorials*, vol. PP, no. 99, pp. 1-1.

[29] D. Giovanelli, B. Milosevic, D. Brunelli and E. Farella, "Enhancing Bluetooth Low Energy with wake-up radios for IoT applications," *2017 13th International Wireless Communications and Mobile Computing Conference (IWCMC)*, Valencia, 2017, pp. 1622-1627.

[30] S. A. Blanchard, "Quick start crystal oscillator circuit," *Proceedings of the 15th Biennial University/Government/ Industry Microelectronics Symposium (Cat. No.03CH37488)*, 2003, pp. 78-81.

[31] S. Iguchi, H. Fuketa, T. Sakurai and M. Takamiya, "92% start-up time reduction by variation-tolerant chirp injection and negative resistance booster (NRB) in 39MHz crystal oscillator," *2014 Symposium on VLSI Circuits Digest of Technical Papers*, Honolulu, HI, 2014, pp. 1-2.

[32] H. Esmaeelzadeh and S. Pamarti, "A precisely-timed energy injection technique achieving 58/10/2μs start-up in 1.84/10/50MHz crystal oscillators," *2017 IEEE Custom Integrated Circuits Conference (CICC)*, Austin, TX, 2017, pp. 1-4.

[33] Joonsuk Lee and Beomsup Kim, "A low-noise fast-lock phase-locked loop with adaptive bandwidth control," in *IEEE Journal of Solid-State Circuits*, vol. 35, no. 8, pp. 1137-1145, Aug. 2000.

[34] W. H. Chiu, Y. H. Huang and T. H. Lin, "A Dynamic Phase Error Compensation Technique for Fast-Locking Phase-Locked Loops," in *IEEE Journal of Solid-State Circuits*, vol. 45, no. 6, pp. 1137-1149, June 2010.

[35] J. Pandey and B. P. Otis, "A Sub-100 μW MICS/ISM Band Transmitter Based on Injection-Locking and Frequency Multiplication," in *IEEE Journal of Solid-State Circuits*, vol. 46, no. 5, pp. 1049-1058, May 2011

[36] J. Zarate-Roldan *et al*., "0.2-nJ/b Fast Start-Up Ultralow Power Wireless Transmitter for IoT Applications," in *IEEE Transactions on Microwave Theory and Techniques*, vol. PP, no. 99, pp. 1-14.

[37] A. Molnar, B. Lu, S. Lanzisera, B. W. Cook and K. S. J. Pister, "An ultra-low power 900 MHz RF transceiver for wireless sensor networks," *Proceedings of the IEEE 2004 Custom Integrated Circuits Conference (IEEE Cat. No.04CH37571)*, 2004, pp. 401-404.

[38] H. Amir-Aslanzadeh, E. J. Pankratz, C. Mishra and E. Sanchez-Sinencio, "Current-Reused 2.4-GHz Direct-Modulation Transmitter With On-Chip Automatic Tuning," in *IEEE Transactions on Very Large Scale Integration (VLSI) Systems*, vol. 21, no. 4, pp. 732-746, April 2013.

978-1-5386-4881-0/18/$31.00 ©2018 IEEE

Authorized licensed use limited to: Texas A M University. Downloaded on May 31,2020 at 00:59:15 UTC from IEEE Xplore. Restrictions apply.